

## Structural and transport properties of epitaxial $\text{Na}_x\text{CoO}_2$ thin films

A. Venimadhav

*Department of Physics, The Pennsylvania State University, University Park, Pennsylvania 16802*

A. Soukiassian

*Department of Materials Science and Engineering, The Pennsylvania State University, University Park, Pennsylvania 16802*

D. A. Tenne and Qi Li<sup>a)</sup>

*Department of Physics, The Pennsylvania State University, University Park, Pennsylvania 16802*

X. X. Xi

*Department of Physics and Department of Materials Science and Engineering, The Pennsylvania State University, University Park, Pennsylvania 16802*

D. G. Schlom, R. Arroyave, and Z. K. Liu

*Department of Materials Science and Engineering, The Pennsylvania State University, University Park, Pennsylvania 16802*

H. P. Sun and Xiaoqing Pan

*Department of Materials Science and Engineering, The University of Michigan, Ann Arbor, Michigan 48109*

Minhyea Lee and N. P. Ong

*Department of Physics, Princeton University, New Jersey 08544*

(Received 16 May 2005; accepted 27 August 2005; published online 20 October 2005)

We have studied structural and transport properties of epitaxial  $\text{Na}_x\text{CoO}_2$  thin films on (0001) sapphire substrate prepared by topotaxially converting an epitaxial  $\text{Co}_3\text{O}_4$  film to  $\text{Na}_x\text{CoO}_2$  with annealing in Na vapor. The films are *c*-axis oriented and in-plane aligned with  $[10\bar{1}0]\text{Na}_x\text{CoO}_2$  rotated by  $30^\circ$  from  $[10\bar{1}0]$  sapphire. Different Na vapor pressures during the annealing resulted in films with different Na concentrations, which showed distinct transport properties. © 2005 American Institute of Physics. [DOI: 10.1063/1.2117619]

Layered cobaltate  $\text{Na}_x\text{CoO}_2$  has attracted much attention recently due to its exceptional properties.<sup>1</sup> It has an unusually high thermoelectric power with low mobility, low resistivity, and high carrier density.<sup>1</sup> The Fermi surface<sup>2</sup> and electrical properties<sup>3</sup> of  $\text{Na}_x\text{CoO}_2$  depend on the Na concentration:  $\text{Na}_x\text{CoO}_2 \cdot 1.3\text{H}_2\text{O}$  is a superconductor for  $x$  around 0.3;<sup>4,5</sup> at  $x=0.5$ , it is a charge-ordered insulator;<sup>6</sup> and at higher Na concentrations it becomes a metal following the Curie–Weiss law.<sup>3,7</sup> The triangular structure of the  $\text{CoO}_2$  planes and the strong electron correlation effect have been recognized as sources of rich properties of  $\text{Na}_x\text{CoO}_2$ .<sup>8</sup> For example, the large thermopower in  $\text{Na}_x\text{CoO}_2$  has been attributed to the spin entropy due to the strong electron correlation effects.<sup>9</sup>  $\text{Na}_x\text{CoO}_2$  has been prepared in polycrystalline and single-crystalline forms, but there are very few reports on  $\text{Na}_x\text{CoO}_2$  thin films.<sup>10–12</sup> Recently, Ohta *et al.*<sup>10</sup> reported epitaxial  $\text{Na}_x\text{CoO}_2$  films by reactive solid phase epitaxy; however, the Na concentration in the films was not well controlled. In this letter, we describe the structural and transport properties of epitaxial  $\text{Na}_x\text{CoO}_2$  thin films fabricated by a process which is similar to that used by Ohta *et al.*,<sup>11</sup> but allows some degree of control of the Na concentration in the film. Films with different Na concentrations showed very different transport properties.

The epitaxial  $\text{Na}_x\text{CoO}_2$  films were fabricated using a two-step process. First, an epitaxial  $\text{Co}_3\text{O}_4$  film was grown by pulsed laser deposition (PLD) on a (0001) sapphire sub-

strate. A KrF excimer laser was used with an energy density of  $3.7 \text{ J/cm}^2$  on a CoO target. The substrate was kept at  $650\text{--}700^\circ\text{C}$  during the deposition in 200 mTorr flowing oxygen. At a repetition rate of 8 Hz, the deposition rate is  $0.11 \text{ \AA/s}$ . The  $\text{Co}_3\text{O}_4$  film was then sealed in an alumina crucible with sodium bicarbonate ( $\text{NaHCO}_3$ ) or sodium acetate ( $\text{NaOOCCH}_3$ ) powder and heated to  $800^\circ\text{C}$  for 2.5 h to form the  $\text{Na}_x\text{CoO}_2$  film. A topotaxial conversion occurred, during which the crystallographic alignment of  $\text{Co}_3\text{O}_4$  was inherited by  $\text{Na}_x\text{CoO}_2$ . The thickness of the  $\text{Co}_3\text{O}_4$  film was around  $1600 \text{ \AA}$ , which became  $\sim 3000 \text{ \AA}$  following the topotaxial conversion to  $\text{Na}_x\text{CoO}_2$ .

X-ray diffraction scans of an epitaxial  $\text{Co}_3\text{O}_4$  film on a (0001) sapphire substrate are shown in Fig. 1.  $\text{Co}_3\text{O}_4$  has a spinel structure with a space group  $\text{Fd}\bar{3}m$ . The  $\theta$ - $2\theta$  scan in Fig. 1(a) shows only peaks arising from diffraction off (111)  $\text{Co}_3\text{O}_4$  planes apart from the substrate peak, indicating a phase-pure  $\text{Co}_3\text{O}_4$  film with [111] direction normal to the substrate surface. The rocking curve of the  $\text{Co}_3\text{O}_4$  111 peak had a full width at half maximum (FWHM) of  $0.24^\circ$  in  $\omega$ , equal to our instrumental resolution. A lattice parameter  $a = 8.087 \pm 0.001 \text{ \AA}$  was obtained. A  $\phi$  scan of the 220  $\text{Co}_3\text{O}_4$  peak is shown in Fig. 1(b), where  $\phi=0^\circ$  is aligned parallel to the  $[10\bar{1}0]$  in-plane direction of the sapphire substrate. The presence of six 220 peaks (where a single crystal would show only three) indicates an epitaxial  $\text{Co}_3\text{O}_4$  film with two twinned variants related by a  $60^\circ$  rotation. The FWHM in  $\phi$  is  $0.55^\circ$ . The in-plane epitaxial relationship is that  $[110]\text{Co}_3\text{O}_4$  is rotated by  $\pm 30^\circ$  from  $[10\bar{1}0]\text{Al}_2\text{O}_3$ .

<sup>a)</sup>Electronic mail: qil1@psu.edu

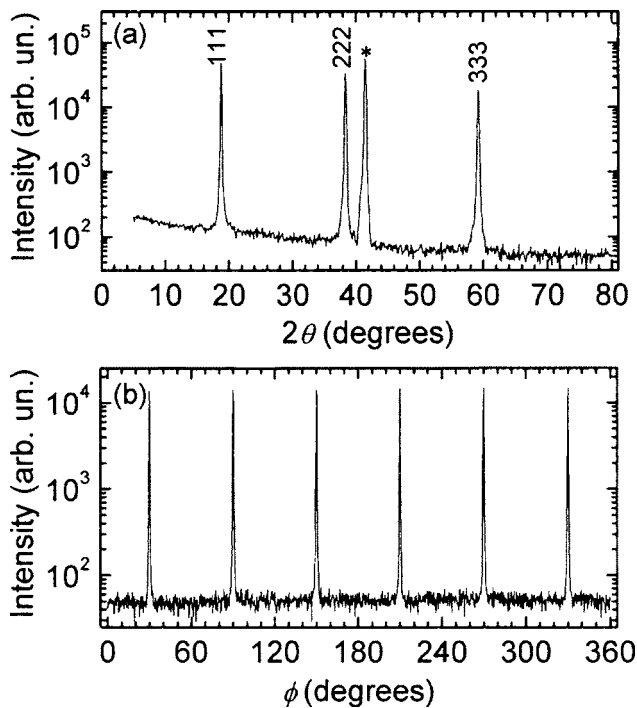


FIG. 1. (a)  $\theta$ - $2\theta$  x-ray diffraction scan of a  $\text{Co}_3\text{O}_4$  film grown on a (0001) sapphire substrate. The 0006 sapphire substrate peak is marked by an asterisk (\*). (b)  $\phi$ -scan of the 220  $\text{Co}_3\text{O}_4$  peak at  $\chi=54.7^\circ$ , indicating that the film is epitaxial.  $\phi=0$  is parallel to the  $[10\bar{1}0]$  in-plane direction of the substrate.

The crystallinity and phase purity of the film after the topotaxial conversion depend sensitively on the annealing conditions. Under the optimized condition (800 °C for 2.5 h), the film is completely converted into  $\text{Na}_x\text{CoO}_2$  without decomposition. X-ray diffraction scans of a  $\text{Na}_x\text{CoO}_2$  film, which was converted from a  $\text{Co}_3\text{O}_4$  film by annealing with  $\text{NaHCO}_3$  powder, are shown in Fig. 2.  $\text{Na}_x\text{CoO}_2$  has a hexagonal  $\text{P6}_3\text{22}$  structure. In the  $\theta$ - $2\theta$  scan in Fig. 2(a),  $00l$  peaks of  $\text{Na}_x\text{CoO}_2$  are observed beside a substrate peak, indicating a  $c$ -axis-oriented film. A weak peak of  $\text{NaHCO}_3$  is also present due to the  $\text{NaHCO}_3$  dust on the film surface resulting from the annealing process, which is also confirmed by a Raman scattering measurement. The  $\phi$ -scan of the  $10\bar{1}2$   $\text{Na}_x\text{CoO}_2$  peak is shown in Fig. 2(b), where  $\phi=0$  is parallel to the  $[10\bar{1}0]$  direction of the sapphire substrate. The six-fold symmetry indicates a topotaxial conversion from the epitaxial  $\text{Co}_3\text{O}_4$  film with the angle between  $[10\bar{1}0]$   $\text{Na}_x\text{CoO}_2$  and  $[10\bar{1}0]$  sapphire being  $30^\circ$ . Lattice constants  $c=11.02\pm 0.003$  Å and  $a=2.456\pm 0.003$  Å were obtained. The rocking curves showed a broad FWHM of  $2^\circ$  in  $\omega$  and  $1.02^\circ$  in  $\phi$ . These values indicate that the crystalline quality of the topotaxially converted  $\text{Na}_x\text{CoO}_2$  film is not as high as that of the starting  $\text{Co}_3\text{O}_4$  film.

Figure 3(a) is a bright-field transmission electron microscopy (TEM) image of a  $\text{Na}_x\text{CoO}_2$  film. It shows the film with a smooth surface. An x-ray energy dispersive spectroscopy (EDS) analysis shows a generally uniform distribution of Na concentration in the film. Occasionally, thin layers of amorphous material, such as the white line shown in Fig. 3(a), occur in the film, which have higher Na concentration than that in the crystalline  $\text{Na}_x\text{CoO}_2$  film. A much thicker amorphous layer, nonuniform and discontinuous, was observed at the film/substrate interface, whose

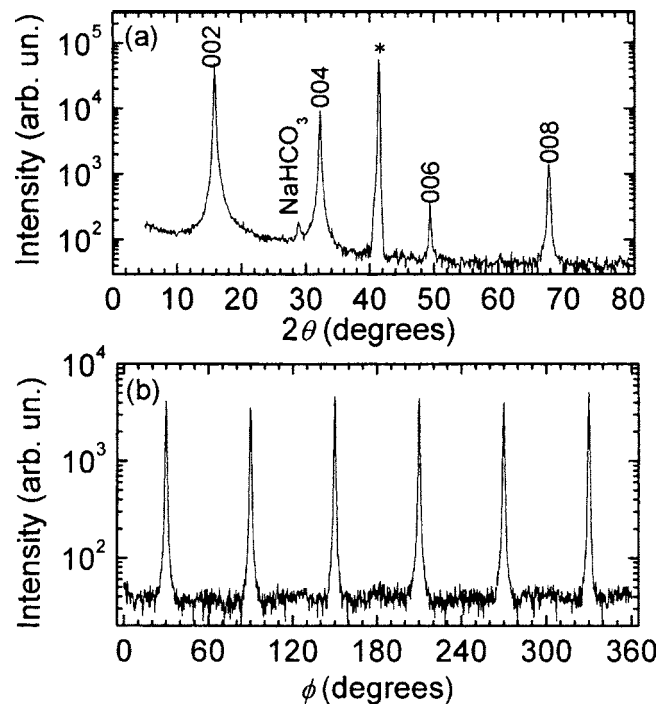


FIG. 2. (a)  $\theta$ - $2\theta$  x-ray diffraction scan of a  $\text{Na}_x\text{CoO}_2$  film on a (0001) sapphire substrate. The 0006 sapphire substrate peak is marked by an asterisk (\*). (b)  $\phi$ -scan of the  $10\bar{1}2$   $\text{Na}_x\text{CoO}_2$  peak at  $\chi=23.6^\circ$ , indicating that the film is epitaxial.  $\phi=0$  is parallel to the  $[10\bar{1}0]$  in-plane direction of the substrate.

chemical composition is similar to the substrate ( $\text{Al}_2\text{O}_3$ ). Figures 3(b) and 3(c) are selected area electron diffraction (SAED) patterns corresponding to the film and the substrate, respectively. They show an epitaxial relationship between the  $\text{Na}_x\text{CoO}_2$  film and the substrate of  $\text{Na}_x\text{CoO}_2(0001) \times [10\bar{1}0] \parallel \text{sapphire}(0001)[2\bar{1}\bar{1}0]$ , which is consistent with the x-ray diffraction analysis. The smeared intensity distribution of reflections in Fig. 3(b) indicates distortions of crystal

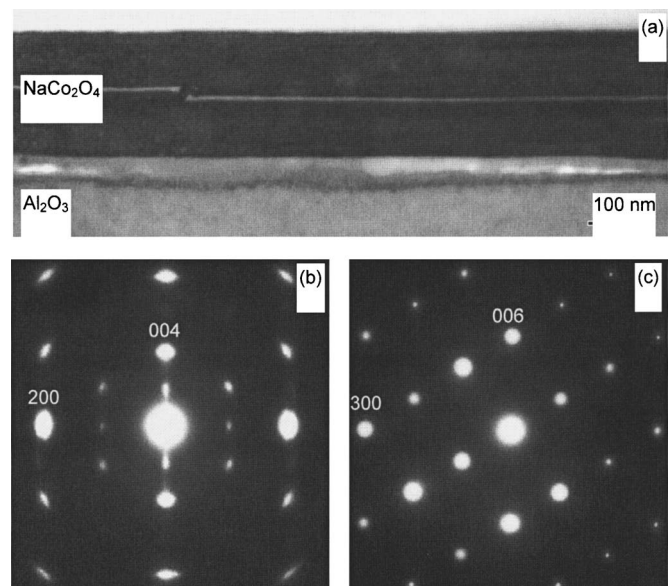


FIG. 3. (a) Bright-field TEM image of a  $\text{Na}_x\text{CoO}_2$  film on a sapphire substrate. The white line in the middle of the film corresponds to a thin layer of Na-rich amorphous material. (b) SAED pattern from the film. (c) SAED pattern corresponding to the substrate.

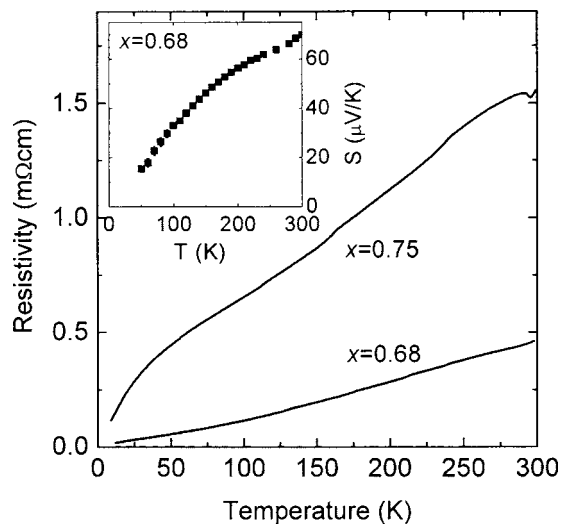


FIG. 4. Resistivity vs temperature curves for two  $\text{Na}_x\text{CoO}_2$  films with different Na concentrations. Inset: Thermopower vs temperature for a  $\text{Na}_x\text{CoO}_2$  film with  $x=0.68$ .

planes in the thin film, consistent with high-resolution TEM observations of waviness in the  $\text{Na}_x\text{CoO}_2$  lattice planes. Details of the microstructure investigation of the  $\text{Na}_x\text{CoO}_2$  films will be published elsewhere.

The Na concentration of the  $\text{Na}_x\text{CoO}_2$  films depends on the powder used for the annealing. At 800 °C, the equilibrium vapor pressure is 0.155 Torr for  $\text{NaHCO}_3$  and 444 Torr for  $\text{NaOOCCH}_3$ . EDS measurements show that the Na concentration is always  $x=0.68\pm 0.03$  for films annealed in  $\text{NaHCO}_3$ . The  $x$  value in films annealed in  $\text{NaOOCCH}_3$  depends on the annealing conditions, and for the optimized condition given above (800 °C for 2.5 h)  $x=0.75\pm 0.02$ . Figure 4 shows the resistivity versus temperature curves of two  $\text{Na}_x\text{CoO}_2$  films with different Na concentrations. The temperature dependence for the film annealed in  $\text{NaOOCCH}_3$ , marked by “ $x=0.75$ ,” is characteristic of bulk and single-crystal  $\text{Na}_x\text{CoO}_2$  samples with  $x=0.75$ .<sup>3,12</sup> The downturn at low temperatures has been attributed to a phase transition to an antiferromagnetic spin-density wave.<sup>13</sup> The resistivity behavior of the film annealed in  $\text{NaHCO}_3$ , marked by “ $x=0.68$ ,” is consistent with single crystals with lower Na concentrations.<sup>3</sup> The inset to Fig. 4 shows the thermopower,  $S$ , versus temperature for a film with  $x=0.68$ . A temperature gradient was generated by a resistive heater attached on one end of the film while the other end was mounted on a cold finger. A pair of type- $E$  (chrome-constantan) thermocouples and a pair of 25  $\mu\text{m}$  gold wires were used to measure the temperature gradient and the difference of electric potential, respectively, to obtain the thermoelectric power. The magnitude of  $S$  at 300 K, as well as the overall temperature depen-

dence shown in the figure, is consistent with the result from the in-plane measurement of single crystals with  $x=0.7$ .<sup>9</sup> These results further confirm the Na concentration measurements by EDS.

In conclusion, epitaxial thin films of  $\text{Na}_x\text{CoO}_2$  were prepared by annealing PLD-grown epitaxial  $\text{Co}_3\text{O}_4$  films in Na vapor. The Na compounds used during annealing,  $\text{NaHCO}_3$  and  $\text{NaOOCCH}_3$ , have different Na vapor pressures, resulting in  $\text{Na}_x\text{CoO}_2$  films of two different Na concentrations. The topotaxial conversion led to a poorer crystallinity in the  $\text{Na}_x\text{CoO}_2$  films than in  $\text{Co}_3\text{O}_4$  films. Nevertheless, the films are  $c$ -axis oriented with in-plane alignment with the substrate. The temperature dependent transport properties are distinctly different for films of different Na concentrations, and they are consistent with the bulk results. Our results demonstrate that some degree of control of the Na concentration in the  $\text{Na}_x\text{CoO}_2$  films can be achieved by using Na compounds of different vapor pressures during annealing.

The work was partially supported by the NSF under Grant Nos. DMR-0405502 (for Q.L.), DMR-0103354 (for X.X.X. and D.G.S.), DMR-0205232 (for Z.K.L.), and DMR-0308012 (for X.P.), by the U.S. DOE under Grant Nos. DE-FG02-01ER45907 (for X.X.X.) and DE-FG02-97ER45638 (for D.G.S.), and by the ONR under Grant No. N00014-04-1-0057 (for N.P.O.).

- <sup>1</sup>I. Terasaki, Y. Sasago, and K. Uchinokura, *Phys. Rev. B* **56**, R12685 (1997).
- <sup>2</sup>P. H. Zhang, W. D. Luo, M. L. Cohen, and S. G. Louie, *Phys. Rev. Lett.* **93**, 236402 (2004).
- <sup>3</sup>M. L. Foo, Y. Wang, S. Watauchi, H. W. Zandbergen, T. He, R. J. Cava, and N. P. Ong, *Phys. Rev. Lett.* **92**, 247001 (2004).
- <sup>4</sup>K. Takada, H. Sakurai, E. Takayama-Muromachi, F. Izumi, R. A. Dilanian, and T. Sasaki, *Nature (London)* **422**, 53 (2003).
- <sup>5</sup>R. E. Schaak, T. Klimczuk, M. L. Foo, and R. J. Cava, *Nature (London)* **424**, 527 (2003).
- <sup>6</sup>K. W. Lee, J. Kunes, P. Novak, and W. E. Pickett, *Phys. Rev. Lett.* **94**, 026403 (2005).
- <sup>7</sup>I. R. Mukhamedshin, H. Alloul, G. Collin, and N. Blanchard, *Phys. Rev. Lett.* **93**, 167601 (2004).
- <sup>8</sup>J. Sugiyama, J. H. Brewer, E. J. Ansaldo, H. Itahara, T. Tani, M. Mikami, Y. Mori, T. Sasaki, S. Hebert, and A. Maignan, *Phys. Rev. Lett.* **92**, 017602 (2004).
- <sup>9</sup>Y. Y. Wang, N. S. Rogado, R. J. Cava, and N. P. Ong, *Nature (London)* **423**, 425 (2003).
- <sup>10</sup>H. Ohta, S.-W. Kim, S. Ohta, K. Koumoto, M. Hirano, and H. Hosono, *Cryst. Growth Des.* **5**, 25 (2005).
- <sup>11</sup>W. D. Si, S. M. Park, and P. Johnson, in *Proceedings of the 2004 MRS Fall Meeting Technical Program* (Materials Research Society, Pittsburgh, PA, 2004), p. 204.
- <sup>12</sup>Y. Krockenberger, I. Fritsch, G. Cristiani, A. Matveev, L. Alff, H.-U. Habermeier, and B. Keimer, *Appl. Phys. Lett.* **86**, 191913 (2005).
- <sup>13</sup>B. C. Sales, R. Jin, K. A. Affholter, P. Khalifah, G. M. Veith, and D. Mandrus, *Phys. Rev. B* **70**, 174419 (2004).